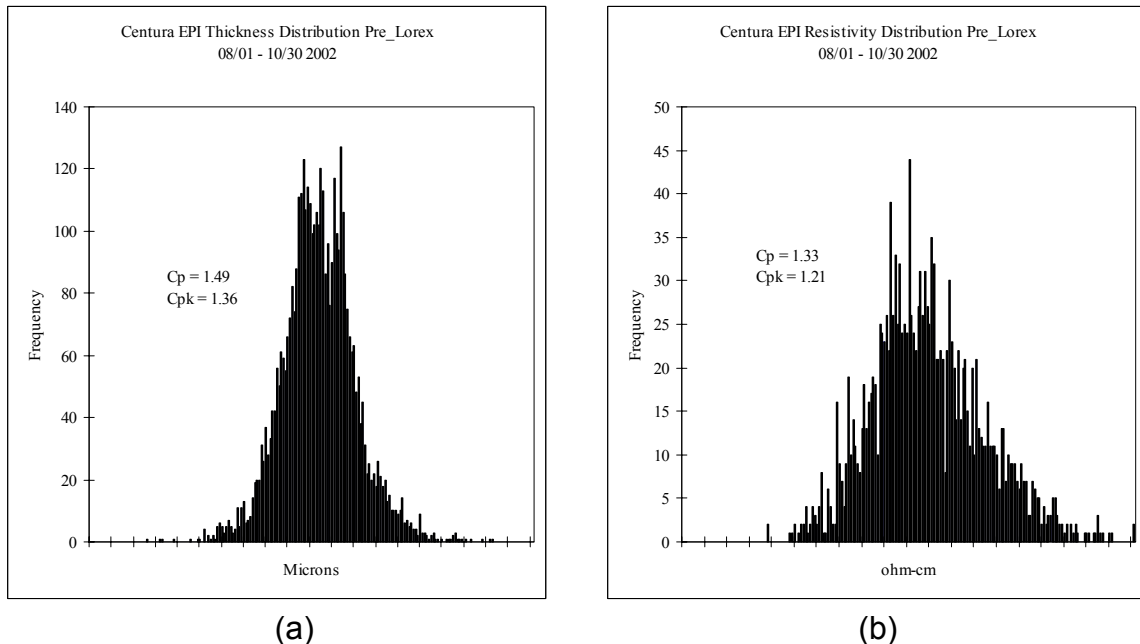


Abstract: *Controlling the Silicon Deposition Rate in an EPITAXIAL process can be a time consuming and difficult activity unless the incoming variables are controlled to very precise levels. TriChlorosilane (TCS) is widely used in the growth of EPITAXIAL silicon. The difficulty with a TCS delivery system is making sure all of the variables of the gas are controlled precisely to deliver a constant grams per minute of TCS to the CVD tool. Here in lies a problem that can be very expensive to eliminate at most EPITAXIAL process facilities. This paper will discuss a unique method of controlling precise grams per minute of TCS delivered to the CVD tool.*

For TI's DFAB 2002 was a year dedicated to improving quality and reducing costs through more efficient manufacturing. The headwater processing step for DFAB's 150 and 200 mm products, the EPI deposition, is currently carried out using 3-chamber Centura's and single chamber ASM tools. The EPI process chemical used is TCS with Hydrogen as the carrier gas. This is a second EPI deposition process on patterned silicon wafers. With increasing demands being imposed TI's specifications for thickness and resistivity, TI found that the performance of the Centuras had become marginally acceptable requiring readjustment of flow rates between every run. This resulted in the tools being idle while the wafers from the previous run went through metrology. Based on the metrology measurements new flow rates were estimated, and entered in the tool. The existing Centura Process capability for both EPI thickness and Resistivity was inadequate to meet the needs of current and new EPI specifications. The two charts below represented the existing Centura Process capability for atmospheric EPI.

Figure 1 a) Thickness distribution and b) resistivity distribution, pre Lorex Piezocon® control of TCS mass transfer rate.

TI saw not only run-to-run control issues, but wafer-to-wafer control issues as well. The Chart below shows wafer-to-wafer variability that was driving overall device performance that was hidden to the Fab.



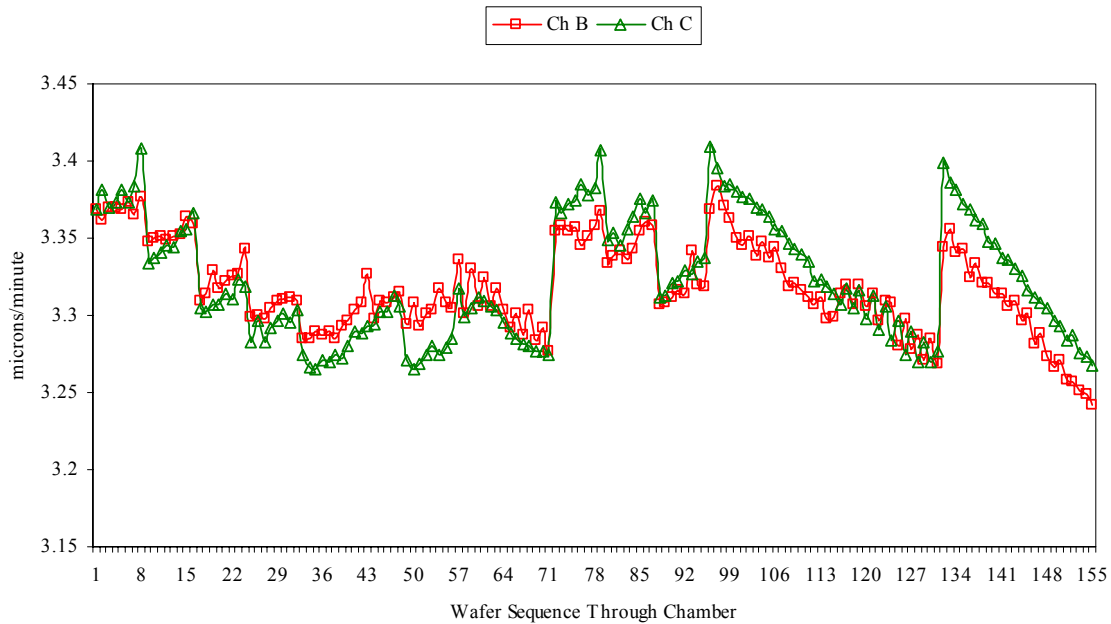


Figure 2 Growth rate for chambers B and C, pre Lorex Piezocon® control of TCS mass transfer rate.

TI's goals were to improve the performance of the Centuras by at least 25%, and reduce the frequency of the manual adjustments in the TCS/H₂ flow rate. To pursue these objectives, TI documented the deposition process and ranked the various exogenous disturbances to the process.

The root causes of thickness variations are drift and instability of the TCS mass transfer rate to the chamber. As with most vapor delivery systems, TI was doing a good job of controlling the mass transfer rate of the carrier gas (the non-critical component) at the price of doing a very poor job of controlling the mass transfer rate of the process chemical.

Figure 3 shows the main components in TI's TCS vapor delivery system. The bubblers are remotely located on another floor and have a capacity of 90 pounds of TCS. Numerous problems are avoided by supplying TCS vapor/carrier gas to the tool rather than supplying TCS in liquid form. The latter method requires costly manifolding on the TCS supply side of the distribution system, invites the possibility of flooding the chamber with chemical, and if the of liquid distribution line is accidentally exposed to atmosphere a time consuming purging process is needed. In estimating the effects of bubbler disturbances on concentration it is useful to express the concentration in terms of pressure ratios as

$$\text{Concentration} = \frac{P_v}{P_{\text{carrier}}} . \quad (1)$$

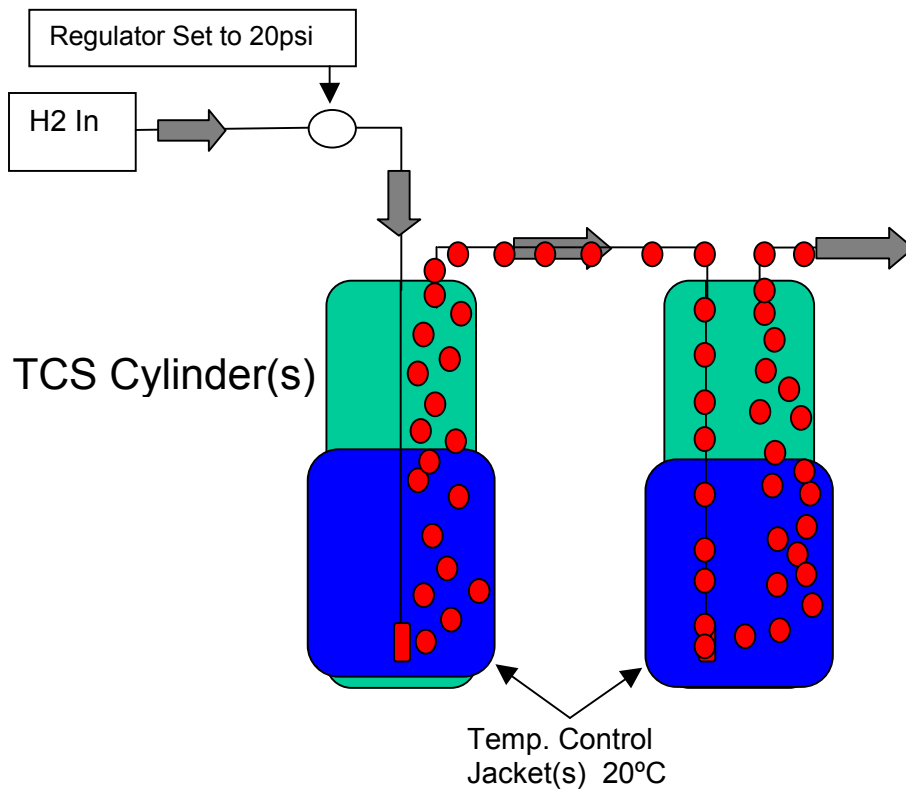


Figure 3 DFAB's TCS bubbler system.

This estimation is possible because of the well-known relationship for estimating vapor pressure as a function of liquid temperature and pressure (Antoine's equation). This relationship is approximately correct in that it ignores the effect of compressibility, i.e., $z \neq 1$, however, it is adequate for estimating the effects of bubbler disturbances on concentration and, in turn, the sensitivity of the mass transfer rates of process chemicals to changes in bubbler temperature or pressure. A more useful form for representing concentration is to express the concentration as a ratio of volumes either as

$$\text{Concentration} = \frac{Q_v}{Q_{Total}} = \frac{Q_v}{Q_v + Q_{carrier}} \quad (2)$$

or

$$\text{Concentration} = \frac{Q_v}{Q_{carrier}} \quad (3)$$

from which the state invariant mass ratios of $Grams_{Chemical} / SL_{Carrier}$ or $Moles_{Chemical} / SL_{Carrier}$ can be calculated (moles are proportional to mass with the constant of proportionality being molecular weight). The benefit of expressing concentration in either of these two forms is that the concentration is independent of the temperature and pressure. That is to say, if the mixture downstream of the bubbler undergoes temperature and/or pressure changes the volumetric ratios will change, but the mass ratios will not.

Elements contributing to exogenous variations in TCS mass transfer rate are:

Variations in Bubbler Temperature:

The important temperature is that of the TCS liquid in the rising column of H₂ bubbles, not the temperature as measured by a bubbler heater controller or thermal well sensor located away from the bubbling column, which can easily differ by several C° from that of the TCS in the column of H₂ bubbles. The temperature of the TCS liquid determines the TCS vapor pressure. Simply put, the vapor pressure is the pressure at which there is an equilibrium between the rate at which TCS molecules are ejected from the liquid phase and the rate at which TCS molecules are reabsorbed by the liquid. The rate of ejection of TCS molecules from the liquid phase is a function of the population of TCS molecules at the liquid/H₂ interface whose thermal energy exceeds that of the van der Waal energy binding the liquid together. Correspondingly, the rate of reabsorption is a function of the density of vapor phase TCS molecules immediately above the surface of the liquid. The widely used relationship used for computing vapor pressure as a function of temperature is Antoine's equation (three, rather than two coefficient form used here):

$$P_v = \frac{760}{1.01325} \times 10^{A - \frac{B}{T+C}}, \quad (4)$$

where P_v is the vapor pressure in torr and T is the liquid temperature in K°. The coefficients A , B and C depend on the chemical and are determined experimentally. NIST gives these coefficients for TCS as: $A=4.21609$; $B=1170$ and; $C=-27$. (NIST's A , B & C give pressure in Bar so the coefficient $760/1.01325$ is used to give pressure in torr.) Figure 4 graphs the Equation 4 TCS vapor pressure as a function of temperature.

The sensitivity of vapor pressure to changes in bubbler temperature is given in Equation A1 in Appendix 1 (first derivative of Equation 4 with respect to temperature) as:

$$P'_v = \frac{dP_v}{dT} = \frac{760}{1.01325} \times \ln(10) \times 10^{A - \frac{B}{T+C}} \times \frac{B}{(T+C)^2} \quad (5)$$

The TCS vapor pressure sensitivity as a function of temperature is plotted in Figure 5. At TI's theoretical bubbler temperature of 293°K the TCS vapor pressure is seen in Figure 4 to be nominally 492.82 torr and the sensitivity to temperature variations is seen in Figure 5 to be 18.76 torr per °K. The analysis for the TCS mass transfer rate sensitivity to temperature changes is given in Appendix A. The results of this analysis are shown in Figure 6. At TI's nominal bubbler operating point of 293°K and 1800 torr The TCS mass transfer rate sensitivity is 5.4% per °K change in bubbler temperature. From Figure 6 it is seen that at a bubbler temperature of 280°K the TCS mass transfer rate will change roughly 5% per °K change in bubbler temperature and, at 300°K, a 1°K change in bubbler temperature will result in a 5.6% change in TCS mass transfer rate.

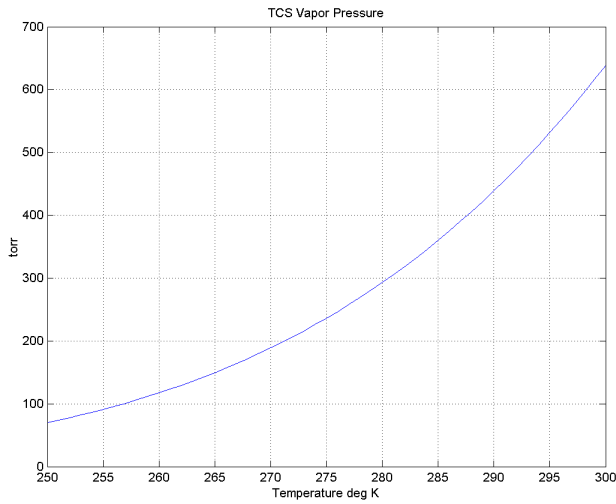


Figure 4 Plot of TCS vapor pressure vs theoretical bubbler temperature

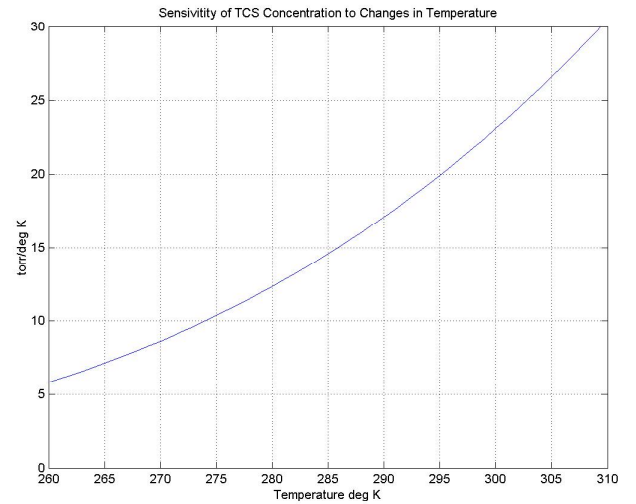


Figure 5 Plot of TCS vapor pressure sensitivity to changes in theoretical bubbler temperature.

Notwithstanding TCS's seeming sensitivity to bubbler temperature, TCS is not one of the more sensitive process chemicals. Some chemicals have a sensitivity of over 20% change in mass transfer rate per °K change in bubbler temperature. And since temperature gradients of several °K within the liquid volume of a bubbler are the norm, better temperature sensors and tighter control of bubbler temperature are not a solution. One example of such gradients can be seen when monitoring the

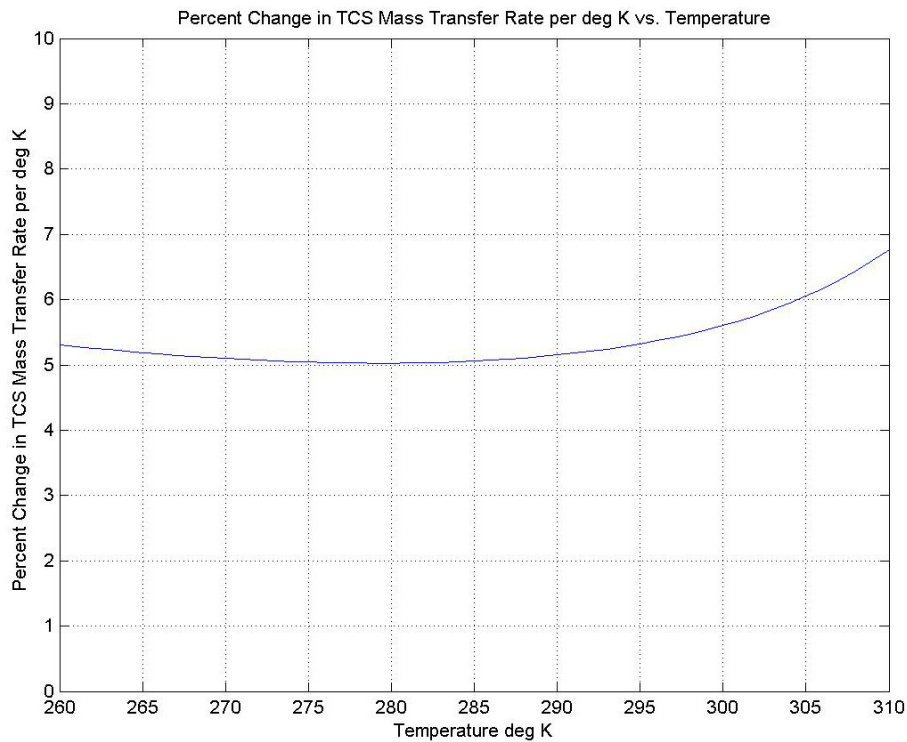


Figure 6 TCS mass transfer sensitivity (percentage change in TCS mass transfer rate per °K) as a function of bubbler operating temperature.

concentration of a temperature-controlled bubbler during and immediately following the onset of bubbling. Assuming the bubbler has been sitting idle, the concentration starts high and slowly drops, eventually reaching an equilibrium point. The time constant involved in reaching equilibrium depends on the size of the bubbler and the carrier gas flow rate. The drop in concentration typically coincides with a several degree decrease in bubbler temperature even though the bubbler's temperature sensor shows that the bubbler is maintaining its temperature set point. The discrepancy arises from the fact that the liquid in the bubbling column is cooled by evaporation. The molecules at the liquid gas interface with the highest thermal energy will have the highest probability of exceeding the van der Waal binding energy of the liquid and transitioning to the vapor phase. This process lowers the average thermal energy of the molecules remaining behind in the liquid, i.e., lowering the temperature of the liquid in the bubbling column, and thus the rate at which the remaining molecules transition to the vapor phase.

Changes in Static Bubbler Pressure:

The bubbler's static pressure is primarily determined by a H₂ pressure regulator located upstream of the bubbler, and is subject to essentially static errors such as drift and maladjustment, as well as dynamic errors resulting from changes in flow rate as the three chambers sequence through their respective process steps. Variations in the carrier gas pressure (equivalent to bubbler pressure when temperature is held constant) directly effect the concentration through Equation 1. Figures 7 and 8 respectively plot the TCS vapor to H₂ partial pressure ratio and TCS concentration as a function of bubbler total pressure at the 20°C operating temperature.

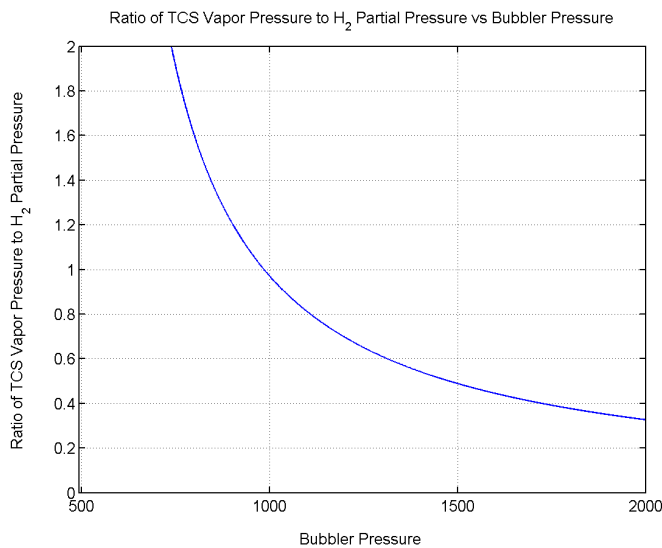


Figure 7 Plot of Ratio of TCS vapor pressure to H₂ Partial Pressure vs bubbler pressure at 20°C operating temperature.

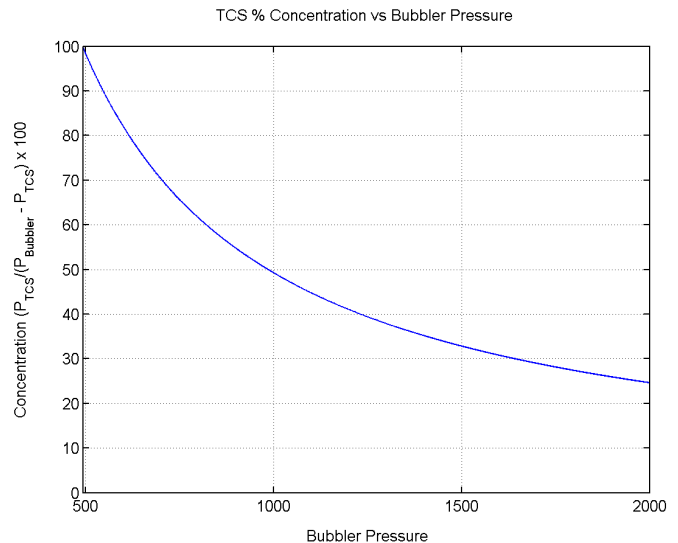


Figure 8 Plot of TCS concentration vs bubbler pressure at 20°C operating temperature.

The sensitivity of TCS mass transfer rate to changes in bubbler pressure is shown in Figure 9 as a function of bubbler operating pressure.

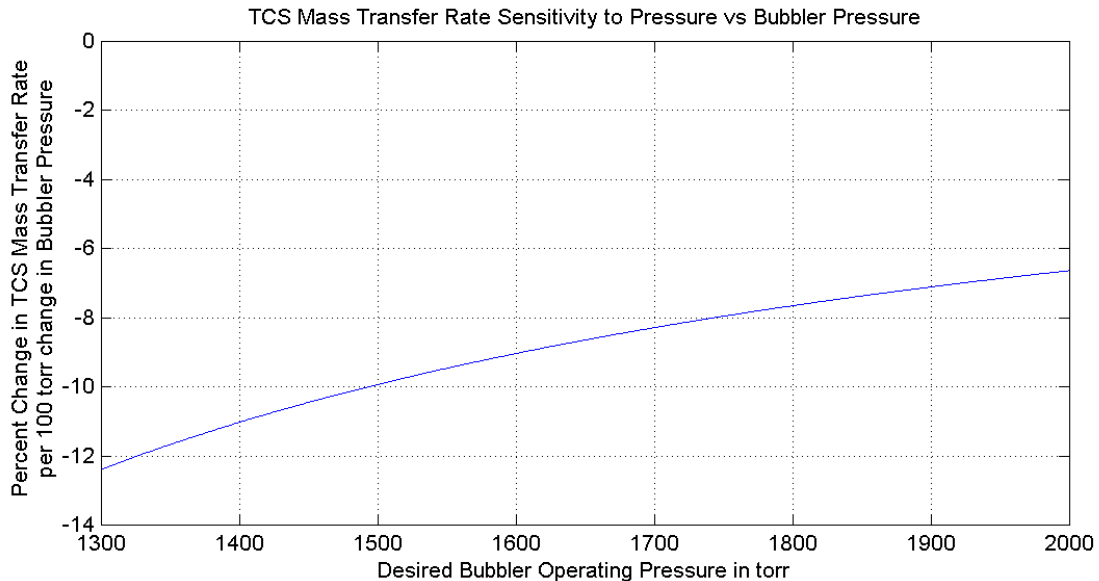


Figure 9 Percentage change in TCS mass transfer rate per 100 torr change in bubbler pressure as a function of bubbler's quiescent operating pressure assuming a fixed bubbler temperature of 20°C.

For example, in Figure 9 it can be seen that at a bubbler pressure of 1800 torr the TCS mass transfer rate will change roughly 7.9% per 100 torr change in bubbler pressure. At a bubbler operating pressure of 1700 torr a 100 torr change in bubbler pressure will result in a 9% change in TCS mass transfer rate. The sense of the negative values for the y-axis is that increases in bubbler pressure will result in decreases in TCS mass transfer rate. (To get the pressure sensitivity per torr change in bubbler pressure, divide the y-axis values by 100.)

Changes in Dynamic Bubbler Pressure:

As the Centura's MFCs call for different flow rates the total TCS/H₂ flow rate changes and this results in second order pressure variations at the bubbler due to the fact that the spring/diaphragm H₂ pressure regulator control does not have infinite gain. As the Centura calls for more flow the head-space pressure in the bubbler drops slightly, thus increasing the concentration of the mixture exiting the bubbler. Figure 10 plots the measured concentration expressed in $Grams_{TCS}/SL_{H_2}$. The data for Figure 10 was recorded by the Lorex Piezocon® Sensor mounted on the Centura immediately upstream of the Centura's three MFCs. The step changes in concentration are a result of the changing MFC set-points as the three chambers step through their respective process cycles. Note that the immediate change in concentration is in the bubbler. The concentration 40' downstream of the bubbler at the Centura's remains unchanged until the new mixture makes its way to the Centura. Because of the rather long distance between the bubbler and the tool there is a time delay between changes in

concentration at the bubbler and when this new concentration reaches the Centura. The amount of delay is a function of the flow rate and the length of tubing between the bubbler and the Centura. Diffusion effects round-off the edges of the step changes.

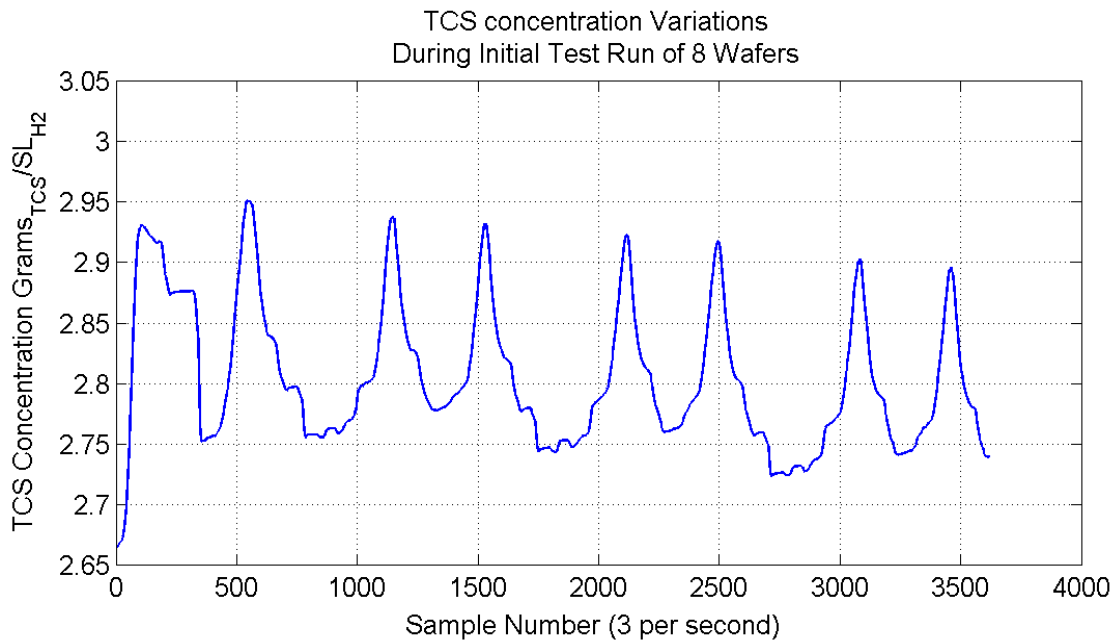


Figure 10 Change in TCS concentration during an 8-wafer test run. Note step changes in concentration due to minor changes in bubbler pressure with flow rate changes. Also note downward trend in concentration as TCS liquid in bubbling column cools slightly due to evaporative cooling.

Variations in Bubbler Liquid Level:

Figure 11 documents the falloff in concentration as a function of bubbler weight/liquid level. This fall off is due to the diminished contact time that the Hydrogen has with the TCS as the liquid level in the bubbler decreases.

These variations in TCS mass transfer rate necessitated a number of cumbersome, monitoring procedures, all of which reduced tool throughput. They included:

1. Need for "Pilots".
2. Measurement of all test wafers for thickness and resistivity prior to beginning another process run.
3. Ongoing manual adjustments of MFC set-points to compensate for changing thickness measurements.

All of these procedures consumed time during which the Centuras were idle.. The need for manual adjustments, coupled with increased reactor qualification time was causing

17% un-planned downtime on the tool. Given the need to increase throughput and overall equipment effectiveness (OEE), a solution to this problem was urgently needed.

Despite the care taken with pilots, 100% measurement and continuous tweaking of MFC set-points, the unacceptable variations in thickness and resistivity were increasing. TI was increasingly sorting quality into its wafers with the attendant drop in yield rather than building quality into its EPI process. In a joint effort with Lorex, TI set about solving this problem.

The solution TI and Lorex implemented was a TCS mass transfer control system using Lorex's Piezocon™ Sensor and Controller. The Piezocon system measures the concentration in units of grams_{TCS}/SL_{H2}, and computes a corrected MFC set point that will compensate for changes in TCS concentration and reestablish the desired TCS mass transfer rate (grams_{TCS}/minute) to each of the Centura's three chambers. A systematic diagram showing the Piezocon Sensor, Controller, Chambers A, B & C's MFCs and their hook up is shown in Figure 11.

These variations in TCS concentration expressed as Grams_{TCS} per Standard Liter of H₂ result in changes in TCS mass transfer rate through the equation:

$$\frac{\text{Grams}_{\text{TCS}}}{\text{minute}} = \frac{\text{Grams}_{\text{TCS}}}{\text{Standard Liter H}_2} \times \frac{\text{Standard Liter H}_2}{\text{minute}} \quad (6)$$

where the last term on the right hand side of Equation 6 is the H₂ carrier gas MFC's flow rate. Thus if the concentration doubled the grams per minute of TCS delivered to the chamber will double if the H₂ mass flow rate remains fixed. However, if the H₂ mass flow rate is correspondingly cut in half then the grams per minute of TCS delivered to the chamber will remain unchanged. The Piezocon Controller makes use of equation 6 to compute a corrected set-point for the MFC that compensates for the changing concentration.

If the tool provides the Piezocon Controller with set-points given specifically in units of grams TCS per minute (as do ASM epsilon tools), then the corrected MFC set-point is found by solving Equation 6 for the Hydrogen flow rate in standard liters per minute.

$$\text{New Set-Point} = \frac{\text{Grams}_{\text{TCS}} \text{ per minute Set-Point}}{\text{Measured Concentration}} = \frac{\frac{\text{Grams}_{\text{TCS}}}{\text{minute}}}{\frac{\text{Grams}_{\text{TCS}}}{\text{Standard Liter H}_2}} = \frac{\text{Standard Liter H}_2}{\text{minute}} \quad (7)$$

That is to say, the new MFC set-point in SLPM is equal to the desired TCS mass transfer rate divided by the measured concentration.

If the tool provides the Piezocon Controller with set-points given as a 0 to 5 Volt MFC set-point (as do TI's AMAT Centura tools), the new MFC set-point is computed as

$$\begin{aligned} \text{New Set-Point} &= \frac{\text{Reference Concentration}}{\text{Measured Concentration}} \times \text{Set-Point Voltage}_{\text{Tool}} \\ &= \frac{\text{Grams}_{\text{TCS Reference}}}{\text{Standard Liter H}_2} \times \text{SLPM}_{\text{Tool}} = \text{Set-Point Voltage}_{\text{New}} \\ &= \frac{\text{Grams}_{\text{TCS Measured}}}{\text{Standard Liter H}_2} \times \text{SLPM}_{\text{Tool}} = \text{Set-Point Voltage}_{\text{New}} \end{aligned} \quad (8)$$

The reference concentration used in Equation 8 is measured by the Piezocon and stored in the Piezocon Controller's EEPROM at the time of installation. This is done through the user interface software provided with each Piezocon. When retrofitting a tool in the field the Piezocon is initially run as a concentration monitor with the tool retaining control of the MFC. The Piezocon user interface software allows the user to display the real-time concentration as a moving graph on a PC screen (like an oscilloscope for concentration). During the initial monitoring the bubbler is run at its nominal operating conditions of temperature pressure and liquid level and the measured concentration is recorded and entered in the set-up window. The concentration should also be compared to the concentration predicted from Antoine's equation. If the discrepancy between the measured concentration and predicted concentration differs by more than, say, 20% there may be a problem with the vapor delivery system such as condensation that should be identified and explained and/or corrected prior to turning control of the MFC over to the Piezocon Controller.

The Piezocon Sensor measures concentration by transmitting a high frequency (MHz) spread-spectrum acoustical signal through the TCS/H₂ mixture. The Piezocon Controller's DSP (TI DSP32C) computes the maximum likelihood time delay between the first received signal and its echo from which the speed of sound in the mixture is calculated and, in turn, the concentration. Included in these calculations is the real-time calculation of the compressibility factor, *z*, of the process vapor. And when the MFC is located down stream of the bubbler these calculations also include a continuously updated gas calibration factor (GCF) for the MFC. By including the real-time GCF in the calculations the Piezocon allows the Hydrogen calibrated MFC's to remain calibrated despite the continuously changing Hydrogen/TCS mixture. The sensor's acoustical signal is transmitted through the nominal 2.5mm thick 316L stainless steel walls of the sensor body and into the flowing gas mixture. Thus, only the flowing TCS/H₂ mixture is in contact with 316L stainless. The Piezocon Controller contains a fixed library of 8 gases, and a user customizable library of up to 32 additional chemicals. The complete Lorex library currently contains over fifty process chemicals from which the user is free to select any 32 chemicals to download to the user library in the Piezocon Controller. Lorex's master chemical library is accessible from Lorex's website where a registered user can click on the desired chemicals and the website will then create a library file containing the chosen chemicals. As new process chemicals

are developed and used Lorex will, upon request, add them to the user's library at no charge. Adding a new chemical to the user library involves creating a chemical parameter file containing the chemical's molecular weight and thermodynamic properties.

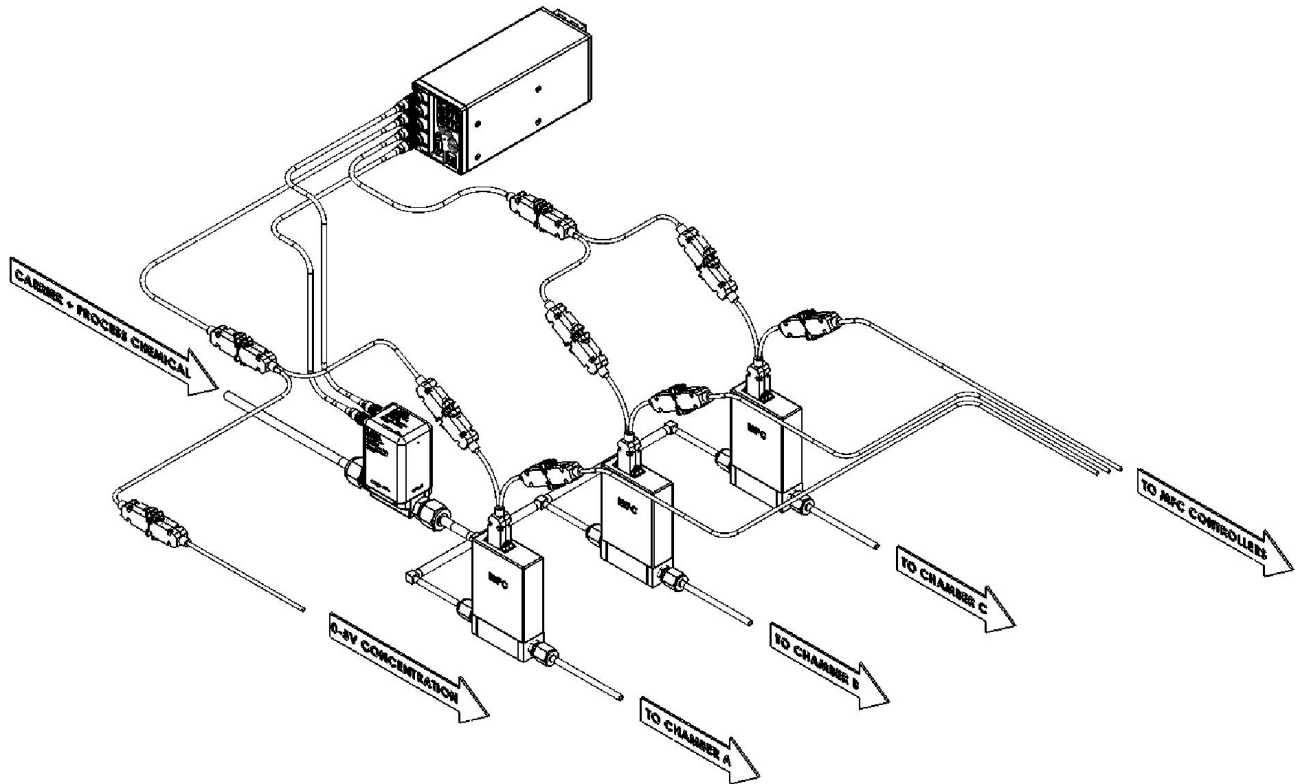


Figure 11 Systematic diagram showing Piezocon Sensor hook-up and its relative location in 3-chamber Centura vapor delivery system.

The initial testing of the Piezocon™ controller was performed on one chamber of a Centura reactor. The sensor was installed in a way that if the results were acceptable it could easily control all three Chambers. After the actual grams/sl was determined the Piezocon™ controller was connected to the TCS Mass Flow Controller (MFC) for Chamber (A), the reactor was then requalified and released back to production. Data was gathered on several initial production lots for wafer-to-wafer variation for EPI thickness. Figure 12 shows a chart of the initial test data that shows the impact of the Lorex Piezocon controller.

This data was so impressive a quick decision was made on the purchase of this system to control all of the Centura TCS process chambers. The initial controller was capable of controlling 2 MFC flows. Lorex made a hardware design change along with a software change that allowed the control of 3 MFC flows from one controller. The new 3-channel controller was purchased and installed on the 1st Centura reactor at the end of September 2002. The 2nd system was installed at the end of October 2002.

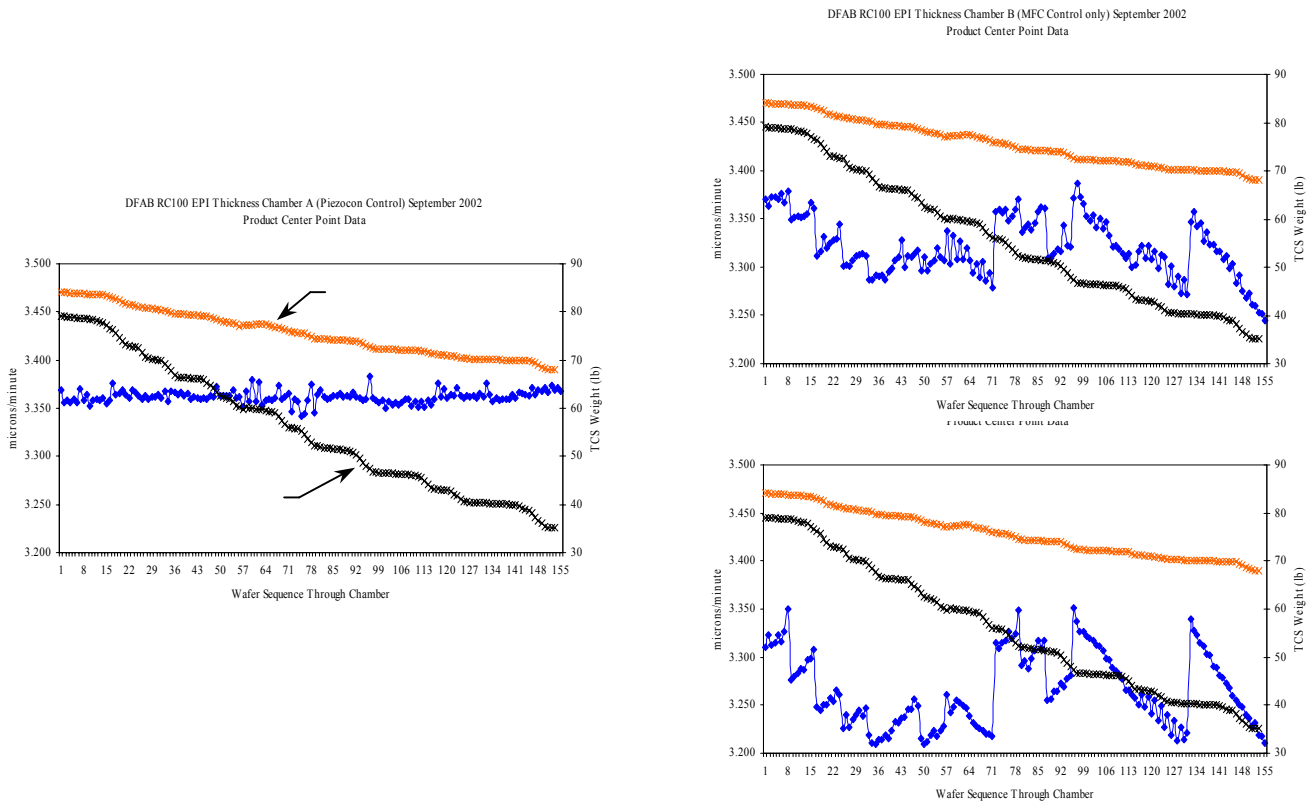


Figure 12 Epi growth rates for chambers A, B & C and TCS cylinder weight versus wafer number. Chamber A's MFC is being controlled by the Piezocon. Chambers B & C's MFCs are controlled directly through the tool and still need continual manual readjustment of the MFC set-points by the operator in order to keep process in bounds, which appear as step changes in growth rates for chambers B & C.

The resulting process control improvement is excellent for the Centura atmospheric EPI process. The Post Piezocon™ EPI thickness and Resistivity distributions are shown in Figure 13. As compared to the Pre Piezocon™ capability there was a 50% improvement in both EPI Thickness and Resistivity capability on the Centura Atmospheric EPI process. The Pre Piezocon™ Thickness Cpk=1.36 and Resistivity Cpk=1.21. The Post Piezocon Thickness Cpk=2.04 and Resistivity Cpk=1.80.

The SPC charts of Figure 14 show the significant improvement that was achieved for not only Thickness control, but Resistivity control as well. The improvement in Resistivity control was expected since we were precisely controlling the EPI growth rate. As the growth rate varies, so does the rate at which the Dopant is incorporated in the silicon layer being grown. By significantly improving the EPI silicon growth rate control TI effectively eliminated a secondary variable that was impacting the overall Resistivity of the EPI layer.

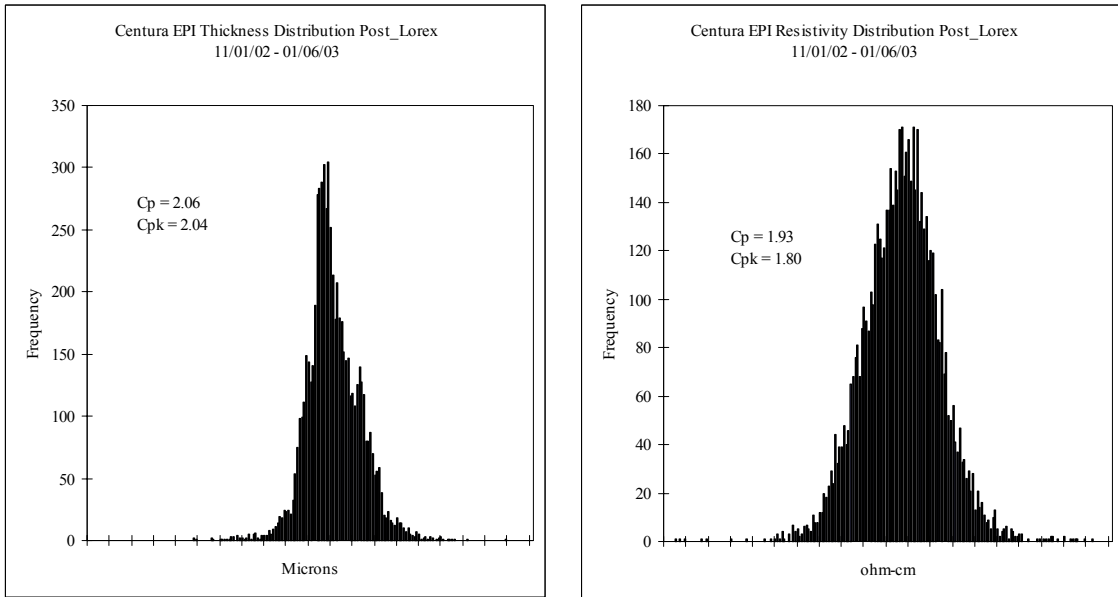
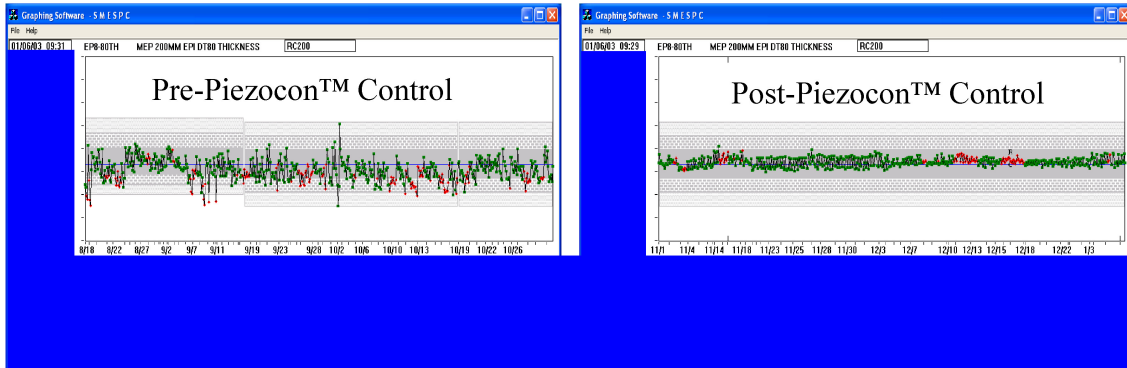
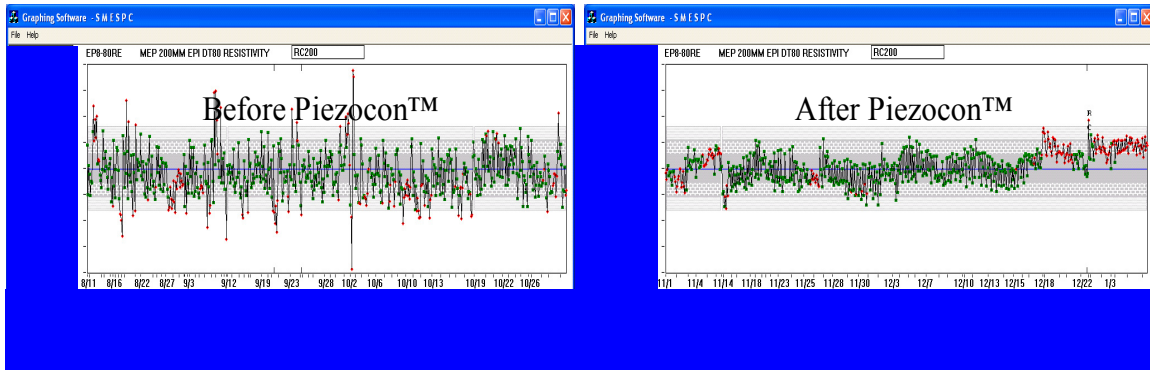


Figure 13 Post Piezocon EPI Thickness and Resistivity distributions.



EPI THICKNESS SPC



EPI RESISTIVITY SPC

Figure 14 Pre and Post Piezocon EPI Thickness and Resistivity SPC.

This type of Process control improvement has significantly impacted the Overall Equipment Effectiveness. Qualification time has been reduced from 17% to 10% of the overall Equipment availability. Qualification time is now driven by Reactor maintenance and Gas bottle changes, rather than manual adjustments required by shifts in EPI thickness and resistivity caused by changes in TCS concentration delivered to the process chamber.

The Lorex Piezocon system has allowed DFAB to test the possibility of using only 1 TCS canister at time to determine the feasibility of an auto-switch system for TCS at DFAB. This would improve equipment availability and reduce the need for gas purges following canister changes. Figure 15 shows the large variability in TCS concentration delivered to the tool during this single canister test. This data is provided by DFAB's TIMS software, which has been connected to the LOREX controller. LOREX provided an analog output for TI's connection. LOREX also provides data connection through an RS232 port or optional DeviceNet and ProfiBus interfaces.

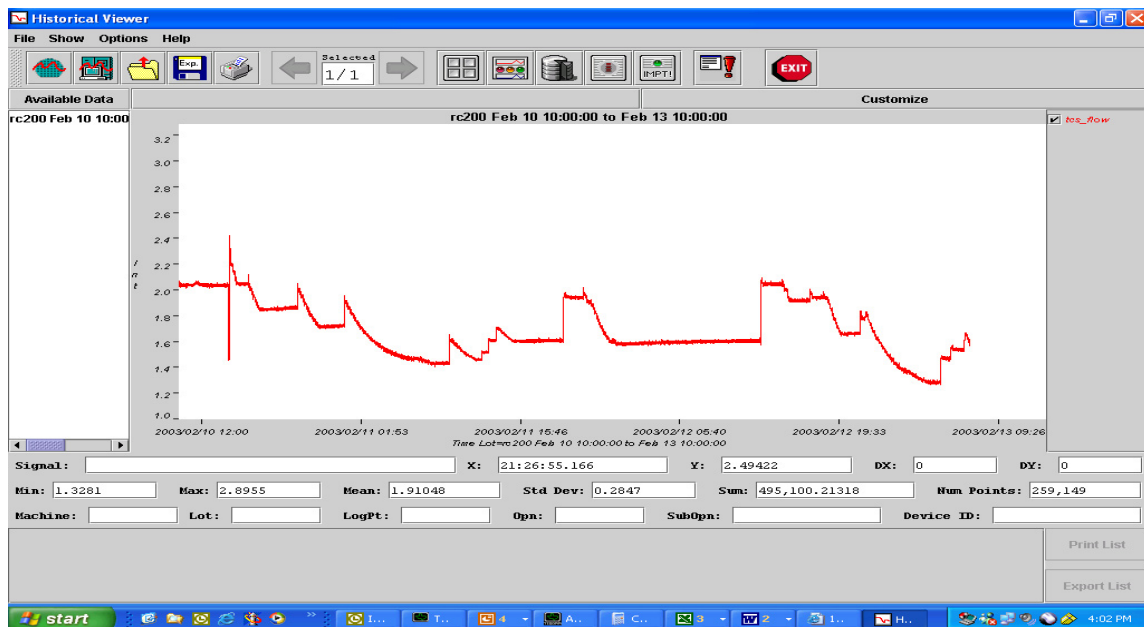


Figure 15 Large variability in TCS concentration when running from a single TCS canister.

The test was run over the Life of the TCS canister (~ 3 days). During this test normal Production was being processed on the EPI CVD tool. The chart below shows the stability of the EPI thickness during the single canister test. With the LOREX Piezocon sensor and controller, no detrimental effect was seen on EPI Thickness control during the test.

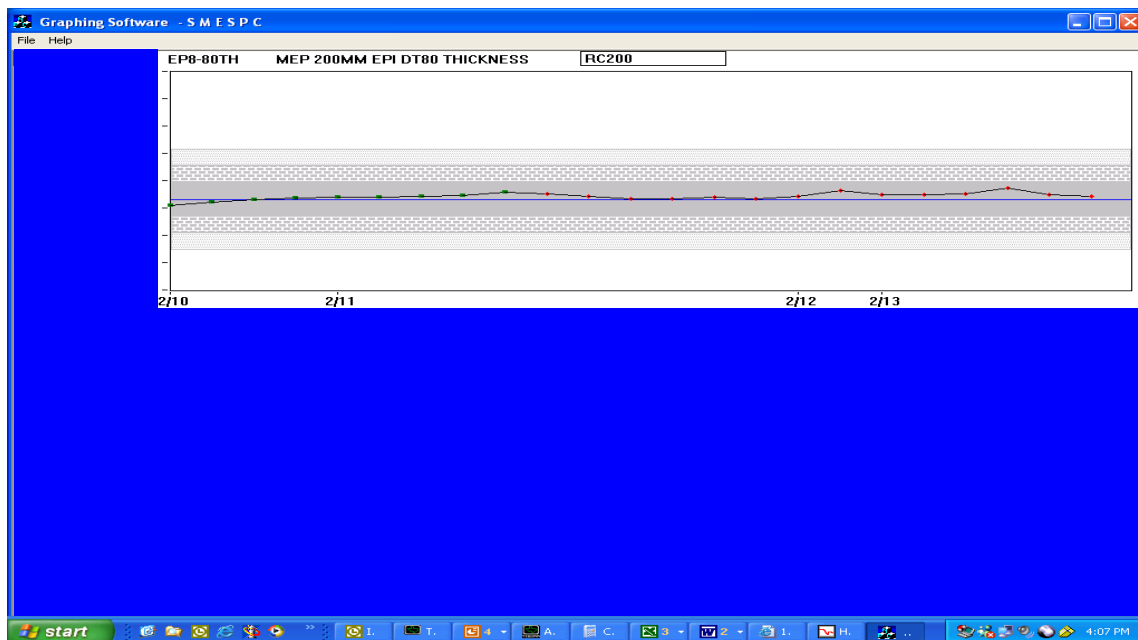


Figure 15 Stability of EPI Thickness during single canister test when Centura's TCS delivery is controlled by the Piezocon.

The impact of the Piezocon™ system on the EPI process, is producing significant interest in other area's of FAB processing. Currently there is another process being tested within DFAB for application of the Piezocon™ system to improve Process control.

Lorex currently has over 600 Piezocon systems operating in the field installed over the past four years and to date the company's return rate is less than one percent. Lorex warranties it's Piezocon Systems for 2 years. Here are the MTBF assumptions and the test results:

1. Assumes a constant failure rate. Failures occur randomly in time and randomly from Piezocon System to Piezocon System.
2. Assumes that this is the failure rate after the initial burn in at Lorex (160 hours @50 deg C) and the failure rate before any end of life effects, so called "wear-out". Because of the resources and length of time that would be involved Lorex has not attempted to get its hands on a wear-out number and use a Weibull distribution.
3. Given assumptions 1 & 2 Lorex chose to use an exponential distribution, i.e.:

$$MTBF = \frac{1}{\lambda} \int_0^{\infty} e^{-\lambda t} dt = \frac{1}{\lambda} \left[\frac{1}{-\lambda} e^{-\lambda t} \right]_0^{\infty} = \frac{1}{\lambda} = \frac{\text{Total Test Hours}}{\text{Total Failures}}$$

4. Given item #3 the Reliability is:

$$Reliability = R = e^{-\gamma t} = e^{-t/MTBF}$$

Lorex's test was on 20 Piezocon Systems under test at 50°C for nominally 19 months (13,879 hours) during which time the company experienced two failures in the electronics only, not the Sensor.

Expressing the MTBF at 20 deg C (typical operating temperature for the Piezocon Controller electronics) the test conditions of 50°C will accelerate the failure rate by a factor of eight (doubles every 10°C). Under these conditions the measured MTBF was 1,109K hours. It should be pointed out that with only two failures the MTBF is a little questionable. For example, if the test had continued and a third unit had failed during the following hour then the calculated MTBF would have dropped to 739.7K hours. On the other hand, if the same 2-failure failure-rate had continued and we had run the test until 10 units had failed and then an eleventh unit failed in the next hour the MTBF would only be reduced to 1,008.7K hours - not much of a decline.

A million plus hours mean time between failures sounds like a long time, so what does it mean to TI? It means the probability that a Piezocon Controller will fail in any given year of operation, is given as:

$$P = 1 - e^{-\frac{8760}{1,109,600}} = 0.00786$$

If TI were operating 20 Piezocons then the probability that one of these 20 Piezocon Controllers would fail in any given year is $20 * 0.00786 = 0.157$ or nominally 16%. As previously mentioned, Lorex warranties the Piezocon for two years.

TI's Piezocon system consists of the Piezocon Sensor and its 1-Channel Controller and cabling as shown in Figure 11. The total cost of the system is less than \$12,000. The 1-channel controller can be ordered with a DeviceNet bus master or slave option for an additional cost of \$350.

APPENDIX A

Bubbler Temperature Sensitivity Analysis:

In the analysis to follow it is assumed for simplicity that the compressibility factor for TCS is unity and not a function of temperature. This assumption will not overly influence the analysis of the process's sensitivity to variations in temperature. The sensitivity of vapor pressure to changes in bubbler temperature is given by the first derivative of Equation 1 with respect to temperature

$$P'_v = \frac{\partial P_v}{\partial T} = \frac{760}{1.01325} \times \ln(10) \times 10^{A - \frac{B}{T+C}} \times \frac{B}{(T+C)^2} \quad (\text{A1})$$

Equation 4 is plotted in Figure 2.

At TI's theoretical bubbler temperature of 293°K the TCS vapor pressure is 492.8227 torr and the sensitivity to temperature variations is 18.7642 torr per °K. At TI's nominal bubbler pressure of 1800 torr the ratio of TCS vapor pressure to carrier gas pressure is

$$R_{293/1800} = \frac{P_v}{P_{carrier}} = \frac{492.8227}{1800 - 492.8227} = 0.37700129 \quad (\text{A2})$$

Holding the total bubbler pressure constant at 1800 torr and increasing the bubbler temperature by 1°K increases the TCS vapor pressure to 511.8757 torr, thus decreasing the carrier gas pressure and increasing the ratio of TCS vapor pressure to carrier gas pressure to

$$R_{294/1800} = \frac{P_v}{P_{carrier}} = \frac{511.8757}{1800 - 511.8757} = 0.39738067 \quad (\text{A3})$$

Thus, for these quiescent operating conditions, a 1°K increase in bubbler temperature will increase the TCS mass transfer rate to the chamber by a factor of

$$\frac{R_{294/1800} - R_{293/1800}}{R_{293/1800}} = \frac{0.39738067 - 0.37700129}{0.37700129} = 0.054025745 \quad (\text{A4})$$

or nominally 5.4%

The sensitivity of TCS mass transfer rate can be expressed more analytically as the derivative of the Pv to carrier gas ratio with respect to temperature

$$\begin{aligned}
\frac{dR_{1800}}{dT} &= \frac{d}{dT} \frac{P_v}{1800 - P_v} = \frac{P'_v(1088 - P_v) + P_v P'_v}{(1800 - P_v)^2 R_{293}} \\
\frac{dR_{1800}}{R_{293}} &= \frac{760}{1.01325} \ln(10) \times 10^{A - \frac{B}{T+C}} \times \frac{B}{(T+C)^2} (1800 - P_v) + P_v \frac{760}{1.01325} \times \ln(10) \times 10^{A - \frac{B}{T+C}} \times \frac{B}{(T+C)^2} \\
&= \frac{\quad}{(1800 - P_v)^2 R_{293}}
\end{aligned} \tag{A5}$$

Multiplying Equation 9 by 100 yields the approximate percentage change in TCS mass transfer rate per degree Kelvin as a function of temperature. This is an approximation because Equation 6 ignores the fact that the compressibility factor for TCS is non-unity and is itself a function of temperature the non unity. Figure 3 plots Equation A5 expressed as a percentage.

Bubbler Pressure Sensitivity Analysis:

Referring to Equation 6 at a bubbler temperature of 293°K and pressure of 1800 torr the ratio of TCS vapor pressure to carrier gas pressure was found to be

$$R_{293/1800} = \frac{P_v}{P_{carrier}} = \frac{492.8227}{1800 - 492.8227} = 0.37700129 \tag{6}$$

This time holding the bubbler temperature constant at 293°K and decreasing the bubbler pressure by 100 torr (~5%) to 1700 torr will increase the ratio of TCS vapor pressure to carrier gas pressure to

$$R_{293/1700} = \frac{P_v}{P_{carrier}} = \frac{492.8227}{1700 - 492.8227} = 0.40824384 \tag{10}$$

Thus, for these quiescent operating conditions, a 100 torr (5%) decrease in bubbler pressure will increase the TCS mass transfer rate to the chamber by a factor of

$$\frac{R_{293/1700} - R_{293/1800}}{R_{293/1800}} = \frac{0.40824384 - 0.37700129}{0.37700129} = 0.082871210 \tag{11}$$

or nominally 8.3%

The sensitivity of TCS mass transfer rate to pressure variations can be expressed more precisely as the derivative of the Pv to carrier gas ratio with respect to bubbler pressure when the bubbler temperature and, hence the TCS vapor pressure is held constant

$$\begin{aligned}
\frac{\frac{\partial R_{293}}{\partial P}}{R_{293/1800}} &= \frac{\frac{\partial}{\partial P} \frac{P_v}{P_{carrier} - P_v}}{R_{293/1800}} = \frac{-P_v}{(P_{carrier} - P_v)^2 R_{293/1800}} \\
&= \frac{\frac{760}{1.01325} \ln(10) \times 10^{A - \frac{B}{293+C}}}{P_{carrier} - \frac{760}{1.01325} \ln(10) \times 10^{A - \frac{B}{293+C}} R_{293/1800}} \\
&= \frac{-492.8227}{(P_{carrier} - 492.8227)^2 0.37700129}
\end{aligned} \tag{12}$$

Multiplying Equation 12 by 100 yields the approximate percentage change in TCS mass transfer rate per torr change in bubbler pressure as a function of bubbler pressure. Again, this is an approximation because Equation 6 ignores the fact that the compressibility factor for TCS is non unity and is itself a function of temperature the non unity. Figure 4 plots Equation 12 expressed as a percentage change per 100 torr.